Macromolecules

Article

pubs.acs.org/Macromolecules

Simple NMR Experiments Reveal the Influence of Chain Length and Chain Architecture on the Crystalline/Amorphous Interface in Polyethylenes

Arifuzzaman Tapash, Paul J. DesLauriers, and Jeffery L. White*

Department of Chemistry, Oklahoma State University, Stillwater, Oklahoma 74078, United States

Supporting Information

ABSTRACT: The distribution of polyethylene (PE) chain segments between the crystalline, noncrystalline, and interfacial morphological regions is an old question that continues to intrigue the polymer science community. Simple solid state NMR experiments described here reveal that even in the case of linear PE, four distinct chain components may be resolved and reliably quantified. The amounts of rigid crystalline chains in all-trans conformations, amorphous chains with increased equilibrium gauche conformer content undergoing essentially isotropic reorientation, mobile all-trans chains (termed mobile trans), and less mobile noncrystalline chains (termed constrained amorphous) can be quantified by simple ^{13}C NMR experiments on solid polymer samples. A version of the EASY background suppression pulse sequence [Jaeger and Hemmann *Solid State Nucl. Magn. Reson.* **2014**, *57*−*58*, 22], modified to eliminate transient Overhauser effects, is used to obtain all of the data in a single experimental acquisition. Using a broad range of well-characterized linear metallocene PE's, the method reveals that the constrained amorphous and the mobile all-trans fractions, i.e., the total interface content, increases essentially linearly with increasing M_w. Topologically modified PE's, at similar M_w's, that contain short-chain branches (SCB), long-chain branches (LCB), or long-chain branches with SCB's (LCB + SCB) have significantly larger interfacial content per unit molecular weight and most significantly so for the LCB + SCB polymers.

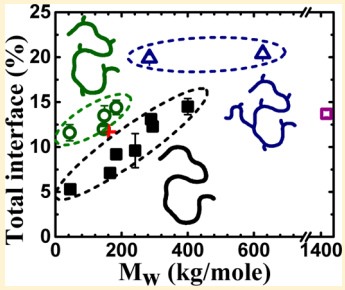

INTRODUCTION

Polyethylene (PE) is the simplest polymer from a chemical structure perspective. That such a chemically simple system still commands the attention of the polymer science community results from relatively complex morphological and physical properties, the variation in those properties depending on the catalytic system used for polymerization, and its myriad commercial applications based on postsynthetic processing options. Much of the renewed interest in PE stems from growing evidence that the interfacial region, or interphase, between the crystalline and noncrystalline amorphous phases is an important factor in controlling final properties. In this contribution, two primary goals are pursued: (1) systematically probe the role of chain length versus chain architecture on the nature and composition of the interface for a series of solid PE's and (2) describe a simple solid-state NMR approach that can quantitatively reveal the types of chains that exist in all PE phases, including the components in the interfacial region.

While the multiple routes to polyethylene production are outside the scope of this work, recent reviews are available,[1−3] and many academic and industrial researchers have experimentally and theoretically interrogated polyethylene morphology and physical properties, in both the melt and solid state.[4−7] Magnetic resonance has proven to be a useful tool for understanding solid-state structure of polyethylene, including linear PE, linear low-density PE copolymers, high-density PE, and ultrahigh-molecular-weight PE (UHMWPE). Methods ranging from static ^1H wide-line methods to relaxation analyses to polarization-transfer ^{13}C site-resolved experiments have been used extensively for the past 30 years to discern the basic phase structure of PE.[8−16] Almost all aspects of the relationships between chain dynamics and relaxation/polarization transfer properties, chain conformation and crystal structure versus chemical shift, quantitative detection of components in one and two dimensions, spin-diffusion, and weaker spin-coupling, as well as connections between NMR responses and mechanical or physical properties, have been explored extensively for PE's.[17,18] A very recent article by Yao and co-workers nicely demonstrates how representative modern solids NMR methodologies can be applied to study phase behavior in UHMWPE.[19]

In parallel with scattering, diffraction, microscopy methods, and the NMR experiments described above, it is now generally accepted that PE phase structure is best described by four components: (a) a primarily orthorhombic crystalline phase with chains in an all-trans conformation, (b) noncrystalline amorphous regions with chains containing a large equilibrium gauche conformer content and which undergo rapid reorientation, (c) chains in all-trans conformations that exhibit increased mobility relative to the crystalline all-trans chains, and (d) chains with equilibrium gauche conformer content whose

Received: March 5, 2015
Revised: April 21, 2015
Published: May 1, 2015

DOI: 10.1021/acs.macromol.5b00475
Macromolecules 2015, 48, 3040−3048

mobility is reduced relative to the amorphous region chains. The latter two chain types are usually assigned as those that together comprise the interfacial region between crystalline lamellae or fibrils and the highly mobile amorphous phase. Additional chain types and phases, such as monoclinic crystalline phases or highly mobile detrital chain fragments, can be generated in drawn fibers.[20−22] The details of the interfacial composition and morphology have become an increasingly important focal point due to the continually increasing variety in the types of PE catalysts used in synthesis, the wider range of comonomers that can be incorporated, and the distinct chain topologies that result. The range of synthesis and processing conditions is so extensive that the need for multiple studies that systematically investigate how key variables such as chain length and chain topology affect interfacial characteristics continues to exist.

Static ^{1}H NMR methods are attractive for studying solid PE, since three of the four components can generally be resolved by analysis of the time-domain signal or relaxation experiments, and domain sizes that agree with scattering methods are accessible using well-established spin-diffusion experiments.[23] Inexpensive benchtop NMR systems can provide access to experiments of this type.[21] ^{13}C methods, while more time-consuming, provide additional information not accessible in the ^{1}H experiments through chemical shift resolution of chain conformations, thereby increasing the resolution and specificity for the four distinct chain types and their domains[24] and also revealing dynamic processes involving chain interconversion between those conformations.[23−26] While not discussed at length here, the chain-diffusion process described by Schmidt-Rohr and Spiess is assumed to be operative in linear PE.[25]

The systematic analysis of the interfacial characteristics of PE as a function of chain length and the number and type of branches, i.e., linear versus short-chain branched versus long-chain branched, is required in order to fully understand the role that the interface plays in final properties and how the interface is defined by synthesis and processing conditions. In this contribution, we use a modified ^{13}C MAS (magic-angle spinning) NMR experiment to quantitatively reveal the amounts of the mobile all-trans chains and the constrained amorphous chains that comprise the interfacial region in linear PE's as a function of chain length and chain topology. Separating contributions from increasing molecular weight and increasingly complex chain architecture was a specific motivating factor in this work, as was the need to acquire the necessary experimental data revealing all four phase components in a single experimental acquisition that can be completed in a reasonable amount of time for typical polyethylenes. A version of the EASY (elimination of artifacts in NMR spectroscopy) background suppression experiment,[27] recently reported by Jaeger and Hemmann, was modified to suppress Overhauser effects such that quantitative subspectra were collected on alternate scans and which when taken together quantify all four phase elements. While the EASY experiment was introduced as a robust background suppression method for solid state NMR, results described here indicate that it has much broader potential to clarify important questions in solid systems, even when background signals are not an issue. Most importantly, the experiment resolves the two components that constitute the interfacial regions. The amounts of the mobile all-trans chains and the constrained amorphous chains in the interface are shown to increase with increasing molecular weight for the linear PE's. The fate of the interfacial components can be followed for PE's with specific introduction of short, long, or long with short chain branches, and results reported here indicate that interfaces in the latter are truly unique compared to linear polymers with the same molecular weight. The spirit of this project is represented by systematically varying chain structures depicted in Scheme 1.

Scheme 1. Schematic Representation of PE Chain Structures Considered in This Study, Ranging from Low Molecular Weight Linear to High Molecular Weight Linear, and Also Including Chains with Short Branches from Alkene Comonomer Incorporation, Long-Chain Branches, and Polymers with Both Long and Short Branches

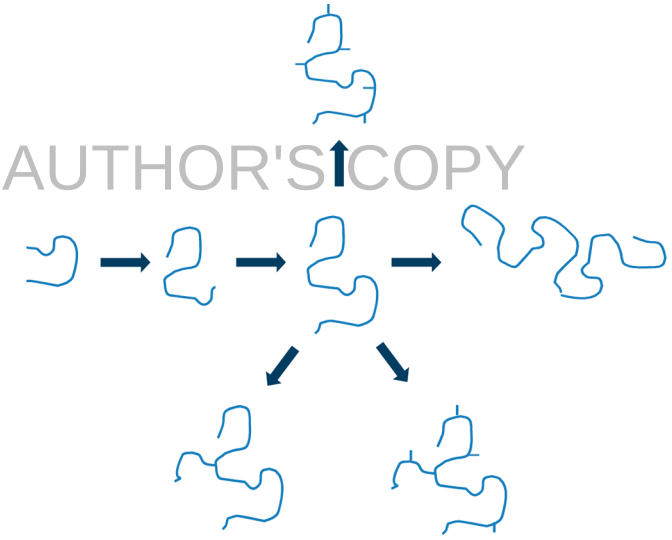

EXPERIMENTAL SECTION

In this study we have investigated 15 well-characterized PE samples of different molecular weight and chain architecture (Scheme 1), ranging from linear, chain with short chain branches (SCB), chain with long chain branches (LCB), and long chain branches containing short chain branches (LCSC), supplied by Chevron Phillips Chemical Co., Bartlesville, OK. Thirteen of the 15 PE's are reactor fluff; those with additional thermal treatments are identified throughout the text. With the exception of the one commercial grade UHMWPE sample (U-1466 in Table 1; obtained from Ticona as GUR4120) prepared via Ziegler−Natta synthesis, all polymers were made using single site metallocene catalysis. Some solvent fractionated materials were also used. Peak temperatures and heat flows were found using a linear integration along the baseline of the peaks. Percent crystallinity was found by taking the heat flow of the initial scan peaks and dividing that by 293 J/g (i.e., heat flow for 100% crystalline PE).[28] The characteristics of the samples are listed in Table 1.

Sample molecular weight and distribution values were measured using a PL220 high-temperature GPC/SEC system (Polymer Laboratories, UK, now an Agilent company) equipped with three HMW-6E columns (Waters Corp., Milford, MA) for polymer separation and a IR4 detector (Polymer ChAR, Spain). Molecular weight determinations were made using Cirrus software (Polymer Laboratories) and the integral calibration method. A broad MWD HDPE Marlex BHB5003 resin (Chevron Phillips Chemical) was used as the broad MW standard. Chromatographic conditions are set as the following: column oven temperature: 145 °C; flow rate: 1.0 mL/min; injection volume: 0.4 mL; polymer concentration: nominally at 2.0−2.5 mg/mL but lower for high MW polymers, depending on samples. In addition to conventional molecular weight measurements, molecular weight and distribution measurements were also made on selected samples using a PL220 GPC/SEC unit coupled to multiangle

DOI: 10.1021/acs.macromol.5b00475
Macromolecules 2015, 48, 3040−3048

Table 1. Description of Polyethylenes Used in This Investigation[a]

sample	M_w (kg/mol)	M_n (kg/mol)	PDI	SCB/ 1000 TC	LCB/ 10000 TC
L-45	45	7	6.4	0	0
L-165	165	57	2.9	0	0
L-184	184	74	2.5	0	0
L-241	241	68	3.5	0	0
L-289	289	63	4.6	0	0
L-294[b]	294	109	2.7	0	0
L-400	400	95	4.2	0	0
U-1466	1466, 2012[c]	261, 412[c]	5.6, 4.9[c]	0	0
SCB-43-h	43	7	6.1	7	0
SCB-146-b	146	127	1.15	12	0
SCB-148-o	148	128	1.15	12	0
SCB-184-o	184	129	1.44	12	0
LCB-152	152, 161[c]	40, 56[c]	4.0, 4.2[c]	0	0.34[c]
LCSC-284-h	284, 417[c]	184, 314[c]	1.5, 1.33[c]	11.9	0.13[c]
LCSC-627-h	627, 1155[c]	458, 1025[c]	1.4, 1.13[c]	11.6	0.10[c]

[a]L = linear; U = UHMWPE; SCB = short chain branch; LCB = long chain branch; LCSC = long chain branch with SCB. All samples are reactor fluff precipitate, with the exception of L294 and U1466. For the polymers with short chain branches, the type of comonomer used to generate the branch is denoted by b = butene, h = hexane, and o = octene. [b]This linear PE was examined following a compression molding step. [c]Obtained via SEC-MALS.

laser light scattering detector (Wyatt) via a heated transfer line as previously described.[29] Short chain branching content in samples was measure using ^{13}C NMR as described by Randall,[30] whereas long chain branching content was obtained from the SEC-MALS method described above.

^{13}C magic-angle spinning (MAS) NMR experiments were acquired using a Bruker DSX Avance 300 MHz instrument on a 4 mm MAS triple-resonance probe equipped with a boron nitride stator. All data reported herein were collected at room temperature with MAS speeds between 5 and 6 kHz, and with ^{1}H decoupling during the acquisition time at rf field strengths ranging from 70 to 100 kHz. Direct polarization was used to generate carbon signals with typical 90° pulse widths of 3.4 μs, and 32 scans were typically collected. To avoid inherent uncertainties about quantitative detection of spins in different phases, cross-polarization was not used in any of the experiments reported here. Unless specifically labeled as single-pulse experiments, all data reported herein were collected using a modified version of the recently reported EASY experiment,[27] which was proposed earlier this year by Jaeger and Hemmann as a convenient method to eliminate troublesome background signals in solid state NMR. Background signals are not an issue for collecting PE spectra on most commercial solids NMR probes, as the PE signals are confined to the narrow 30–35 ppm range of the spectrum. However, as will be explained in detail in the Results section, the experiment is based on an inherent T_1-filter design, which is obviously applicable to systems containing components with large spin–lattice relaxation (T_1) differences. It is well-known in the literature that the amorphous or noncrystalline phase in PE has a very short ^{13}C T_1 value, on the order of a few tenths of a second, while the all-trans crystalline chains typically have T_1 values ranging from 50 to 500 s.[16,24,31] For this reason, T_1 discrimination is often the method of choice for getting amorphous or mobile-only signals in the ^{13}C spectrum. Conversely, the total quantitative spectrum can only be obtained by waiting $5T_1$ between signal acquisitions. In appropriately collected data, one can obtain the spectrum corresponding to only the crystalline chains by taking the difference between a long delay, i.e. $5T_1$, and short delay set of experiments, e.g. a 1 s recycle, as the rapidly relaxing (presumably amorphous) signals would be eliminated. The EASY experiment allows such a series of acquisition to take place, but in a single experimental acquisition where long- and short-relaxation delay spectra are acquired on alternate scans. All of the data are collected simultaneously, thereby minimizing complications inherent to collecting two separate experiments; as such, it is a perfect candidate for collecting all of the required data necessary to discern the composition of all four phases in PE in a single experiment. In the originally published form of the experiments, there is insufficient time to allow all ^{1}H magnetization in highly mobile phases to return to equilibrium following the first decoupling period. In our modified version, a series of ^{13}C 90° saturation or "spoiler" pulses are inserted between the first and second acquisition, as shown in Figure 1. This prevents transient heteronuclear NOE contributions

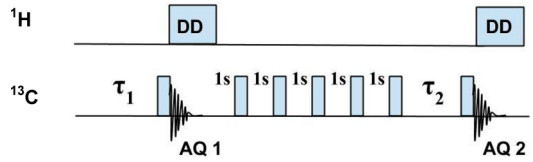

Figure 1. Pulse sequence diagram for the modified-EASY experiment, in which ^{13}C saturation pulses have been inserted between the first and second acquisitions to eliminate transient Overhauser effects and ensure carbon magnetization that has undergone only 1 s of spin–lattice relaxation is accurately sampled. While five saturation pulses were used for most of the data reported here, one is sufficient. All ^{13}C pulses shown are $\pi/2$ pulses. The total sequence as written is repeated n times for signal averaging, with n = 32 for the data reported herein, τ_1 = 2000 s, and τ_2 = 1 s.

from artificially enhancing the intensity of the signals arising from the isotropically reorienting protons in the highly mobile amorphous phase, as ^{1}H T_1's for highly mobile chains in PE are on the order of a second. The first four spoiler pulses on the carbon channel are not necessarily required; as long as there is a single ^{13}C 90° pulse between the first and second acquisition and a comparable 5 s delay, any residual carbon magnetization arising from transient NOE's is eliminated, and only polarization created by 1 s carbon spin–lattice relaxation is sampled in the second free induction decay. Identical results were obtained using only one ^{13}C 90° spoiler pulse. In this way, quantitative signals from all chains in all PE phases, and signals from only the mobile PE chains (including mobile all-trans chains as well as the highly mobile amorphous chains), are collected on alternate scans and stored in separate data buffers. As will be described in detail below, the difference in these two signal sets corresponds to crystalline chains and resolved signals for chains rich in trans–gauche conformers but whose mobility is reduced relative to the mobile amorphous chains, i.e., the constrained amorphous regions in the interface. Standard deconvolution of the transformed spectra using only four signals corresponding to each of the four physical components, and whose chemical shifts agree with control experiments, provides a quantitative distribution of the phases in the PE of interest.

RESULTS AND DISCUSSION

Molecular weight dependent contributions to interfacial morphology were addressed by examining several linear polyethylenes spanning almost 1 order of magnitude in M_w, i.e., 45K–400 K, using a combination of simple one-pulse experiments and the modified-EASY experiment shown above. Figure 2 shows the quantitative single-pulse spectra, acquired using a 2000 s recycle delay, of three of the linear PE's listed in Table 1. As has been observed many times in the literature, two major peaks are observed depending on the percent crystallinity, with the ca. 33 ppm peak often assigned to the crystalline fraction and the ca. 31 ppm peak assigned to the amorphous fraction. However, this is an incomplete designation; the downfield peak arises from chains in an all-trans

DOI: 10.1021/acs.macromol.5b00475
Macromolecules 2015, 48, 3040–3048

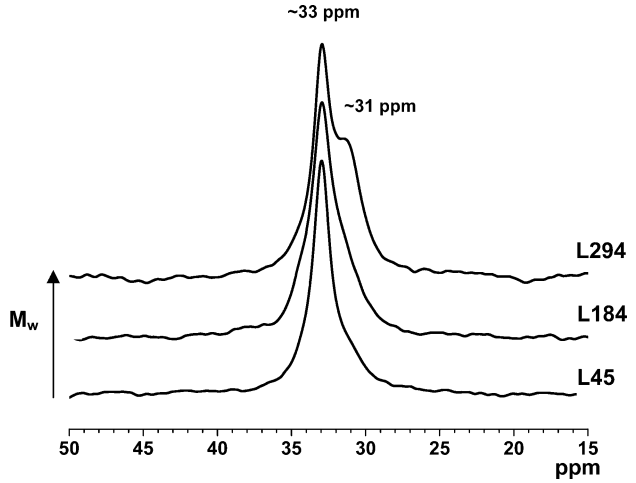

Figure 2. Quantitative single-pulse ^{13}C MAS spectra acquired with a 2000 s recycle delay and high-power ^{1}H decoupling for a subset of the linear PE series listed in Table 1.

conformation and the upfield peak from chains with an increased equilibrium concentration of mixed trans−gauche conformations.[32−34] Whether or not all-trans chains appear only in the rigid crystalline region cannot be discerned from a simple experiment like that shown in Figure 2. Clearly, the fraction of chains with increased gauche conformer content increases with increasing PE molecular weight, and while one might be tempted to simply deconvolute the total line shape using two components to assign percent crystallinity, this has been shown to be an incomplete representation of PE systems.[19,31]

Acquiring spectra with much shorter recycle delays, i.e., in the regime of incomplete spin−lattice relaxation, reveals that heterogeneity exists even in simple linear PE's. Figure 3 compares short (1 s) versus long (2000 s) recycle delays for two different linear PE's; the individual spectra were acquired in separate experiments. In contrast to the long-recycle spectra, the short-recycle spectra are dominated by signals from the amorphous chains. Surprisingly, the short-recycle spectra also contain obvious downfield signal components from chains in all-trans conformations, indicating that all-trans chains exist whose reorientational amplitudes and correlation times approximate those found in the chains of the mobile amorphous phase.

The long- and short-relaxation time traces for the two linear PE samples are quite different, even though the M_w values are almost identical. The apparent increase in the trans−gauche amorphous component at ca. 31 ppm in the 294 K polymer results from a different thermal history compared to the 289 K material; the former was cooled quickly by forming a pressed plaque from the melt while the latter was the as-prepared reactor fluff, which never sees any heat treatment. Note that the crystalline peak chemical shift serves as an internal reference, as it is constant for each sample spectrum. However, the ca. 0.5 ppm difference between the chemical shift of the amorphous trans−gauche signal (31.8 vs 31.2) in the 1 s recycle spectra is real and reproducible in multiple experiments. The differences in the amorphous component chemical shifts cannot be reliably discerned in a simple quantitative single-pulse spectrum, like those shown in the top trace of Figure 3 for L289, as too much uncertainty exist in assigning or fitting such a weak shoulder on the main peak. This result indicates that the rapidly cooled L294 PE either has an amorphous phase characterized by chains with a higher equilibrium gauche fraction than in the L289 PE, as the amorphous peak is more resolved in the L294 case, or experiences differences in chain packing that can contribute to changes in the chemical shift.[32−34] In addition, the possibility that intermediate conformational angles in regions of strain cannot be discounted. Acquiring ^{13}C NMR spectra at long and short recycle delays is not new. However, the power of the T_1 selection is illustrated here for similar M_w samples with different thermal histories and, perhaps more importantly, clarified for the reader as acquisition of long- and short-recycle spectra in a single experiment forms the basis of the modified-EASY experiment that will be described below to elucidate chain length and architecture contributions to interfacial behavior.

The existence of all-trans chain segments with apparent T_1's, and possibly chain dynamics, comparable to conformationally dynamic amorphous chains is better demonstrated by imposing a more stringent T_1 filter. Figure 4 shows compares a series of

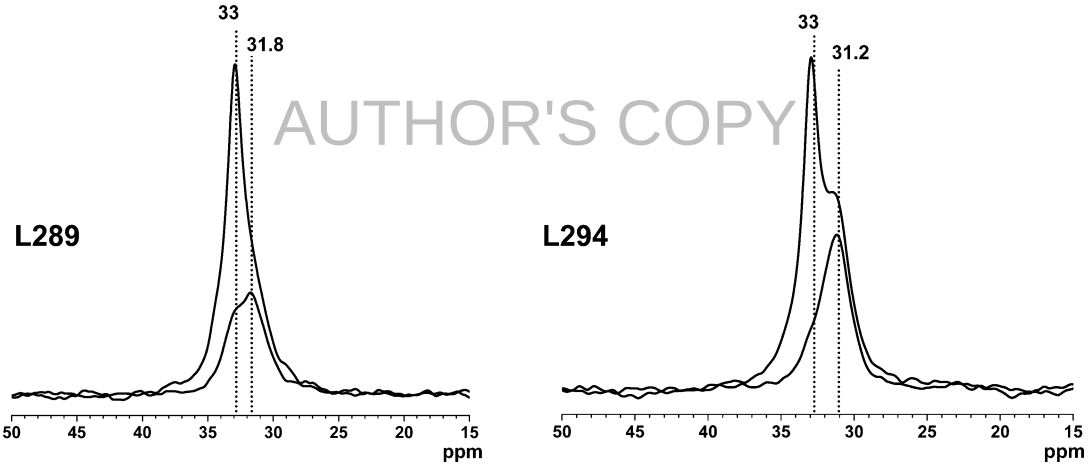

Figure 3. Quantitative single-pulse ^{13}C MAS spectra acquired with a 2000 s recycle delay (top trace) and, in separate experiments, a 1 s recycle (bottom trace) for two linear PE's at similar M_w. Both spectral traces for each sample differ between the two polymers, even though the molecular weight is similar (289 K vs 294 K). However, the thermal history for the two is different; the sample on the right was rapidly cooled from the melt by forming a compression-molded plaque, while the sample on the left is the reactor fluff.

DOI: 10.1021/acs.macromol.5b00475
Macromolecules 2015, 48, 3040−3048

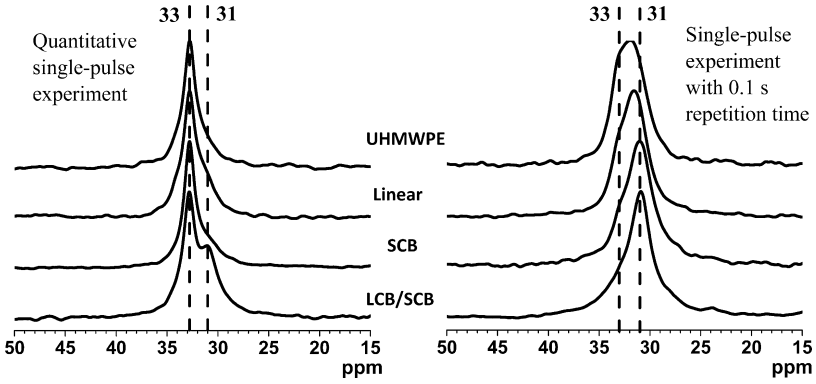

Figure 4. Quantitative single-pulse spectra (left column) and spectra acquired with 0.1 s recycle delay (right column) for four different PE chain types. Specifically, from top to bottom, the samples are listed in Table 1 as U1466, L184, SCB43, and LCSC284. The limiting chemical shifts of 31 and 33 ppm are observed in all spectra.

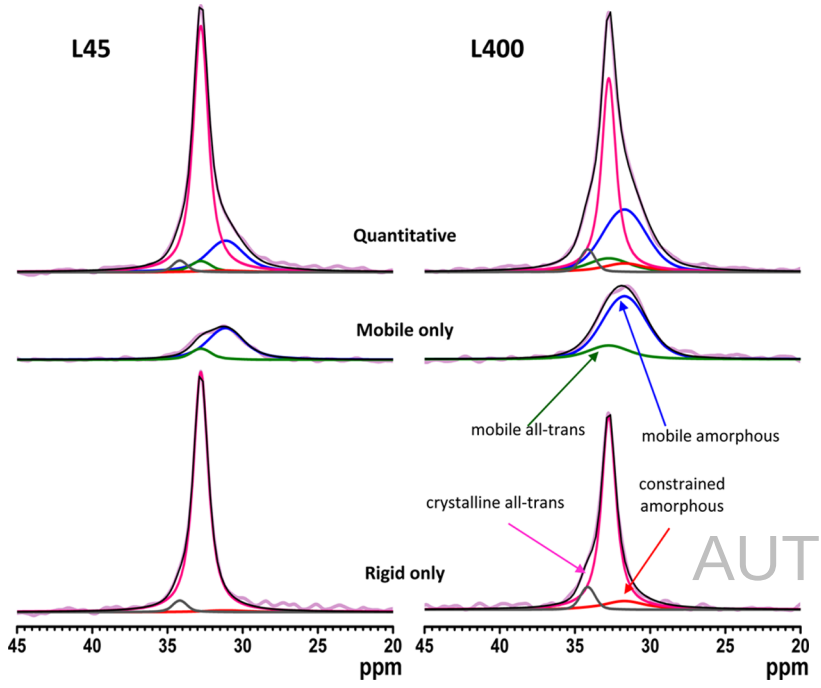

Figure 5. Spectral results from modified-EASY experiment, demonstrating fitting of quantitative 2000 s EASY spectra (top row) based on extraction of individual components from short delay mobile-only spectra (middle row), and the rigid-only difference spectrum (bottom row) of samples L-45 (left column) and L-400 (right column). For clarity, the individual components are identified only on the L-400 PE, but the same assignments apply to all other PE's. In all spectra, the most intense red line component at 32.9 is the signal from crystalline chains, while the blue trace at 31.7 ppm is from chains in the mobile amorphous phase. The smaller red trace and the green trace represent the intensity from the interface, i.e., constrained amorphous 31.7 ppm and all-trans mobile chains at 32.9 ppm, respectively. The small black trace at 34 ppm is from a monoclinic crystalline component, which appears in many, but not all, samples. Individual components are extracted from the mobile-only and rigid-only subspectra and then used without modification to fit the quantitative spectrum in the top row. Note the excellent agreement of the fit.

quantitative single-pulse and 0.1 s recycle time spectra for a wide range of PE chain types, including linear, SCB, LCB, and UHMW PE's. This delay is an order of magnitude shorter than some of the data shown in Figure 3. Of particular interest are the 0.1 s recycle spectra in the right column, all of which contain a clear all-trans signal contribution near 33 ppm. This observation indicates there are all-trans chain segments undergoing fast anisotropic reorientation on a time scale similar to that of the most mobile trans−gauche chain conformers in the amorphous region. The line shape for the UHMWPE and linear PE samples are markedly different in the 0.1 s recycle spectra when compared to the comparable SCB and LCB/SCB spectra. The apparent chemical shift of the amorphous trans−gauche signal varies from 31.8 to 31.1 ppm in the 0.1 s recycle spectra for the different PE types in Figure 4. This result indicates one of two situations: (1) the average gauche fraction of the mobile amorphous chains is lower for the UHMWPE and linear PE relative to the other two chain topologies, or (2) mobile all-trans chains are undergoing fast exchange with trans−gauche chains in the UHMWPE, and to a lesser extent in linear PE, but are not doing so for the SCB and LCB/SCB polymers. Given that clear all-trans chain signals are still discernible at 33 ppm in the UHMWPE and linear PE 0.1 s recycle spectra, the former explanation is most reasonable and is consistent with the trans−gauche conformer shifts discussed above in Figure 3 for spectra obtained with a 1 s recycle delay

DOI: 10.1021/acs.macromol.5b00475
Macromolecules 2015, 48, 3040−3048

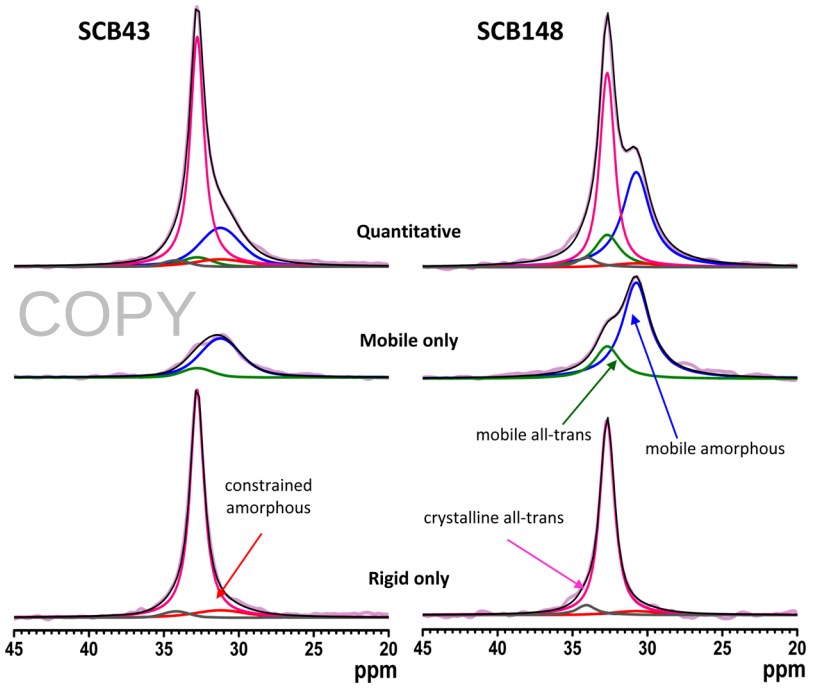

Figure 6. Spectral results from modified-EASY experiment, using the same component analysis procedure described in the text and in the Figure 5 caption. Shown in this example are the quantitative 2000 s EASY spectrum (top row), short delay mobile-only spectrum (middle row), and the rigid-only difference spectrum (bottom row) for short-chained branched PE SCB-43 (left column) and SCB-148 (right column). The individual components are labeled as in Figure 5.

for two linear PE's of the same molecular weight but different thermal processing sequences. Recall in Figure 3 a 31.2 ppm shift was observed for trans−gauche chains in the linear PE rapidly cooled from the melt, while a 31.8 ppm shift was observed for the reactor product. We can conclude from both Figure 3 and Figure 4 that the fast recycle time experiments reveal either differences in the average gauche fraction of chains in the nominally amorphous, but strictly speaking trans−gauche regions of the PE, or possibly differences in chain packing in the amorphous regions as described above. Such differences are detectable for PE's at the same molecular weight but different thermal histories as well as for different PE chain architectures.

The data described above, as acquired using separate quantitative or T_1-filtered acquisition conditions, are insufficient to quantitatively measure all four phase components. However, if taken together in the single modified-EASY experiment shown in Figure 1, the amounts of phases with all-trans crystalline, mobile all-trans, constrained amorphous, and mobile amorphous chains can be defined. Here, the interface/interphase is defined as the combination of the mobile all-trans and constrained amorphous chains. Figure 5 (linear PE) and Figure 6 (SCB PE) show examples of the results from this approach, in which the total spectrum from quantitative 2000 s recycle acquired in the first scan (top), the 1 s T_1-filtered acquisition selecting for mobile components in the second scan (middle), and their difference revealing signals from the crystalline all-trans and constrained amorphous phases (bottom). It is worth mentioning here that the choice of a 1 s delay time for the second portion of the EASY experiment is somewhat arbitrary but does reflect a reasonable starting point for ^{13}C T_1 discrimination in semicrystalline polymers based on historical data.[16,24,31] One might expect a distribution or gradient in polymer chain relaxation behavior as the interfacial region between crystalline and amorphous domains is traversed, as suggested by the 0.1 s recovery data shown in Figure 4. In future work, we will attempt to probe this by exploring a pseudo two-dimensional (2D) version of the EASY experiment, in which the τ_2 value shown in Figure 1 is incremented. While this pseudo-2D EASY would be an extremely long experimental acquisition, and difficult to practically implement for a large sample set like used in this study, it could potentially provide insight into dynamic gradients across the interface in suitably selected materials based on T_{1C} gradients.

Returning again to the example raw data in Figures 5 and 6, individual line shape components are assigned to each of the four physical components in PE described above and one additional component for the monoclinic crystalline signal when applicable. However, fitting those four components to the total quantitative line shape from the 2000 s EASY spectrum does not occur until the last step of the data analysis. Thus, we do not attempt to extract four or five distinct line shape components from such a poorly resolved spectrum. Rather, the 1 s "mobile amorphous" EASY spectrum is fit first (middle trace in Figures 5 and 6), using only the two components, which are physically assignable to regions of PE. The two components are centered at the known chemical shifts for the all-trans PE segments and the amorphous PE component, at ca. 33 and 31.6 ppm, respectively. There is some slight variation in the peak maximum for the amorphous components from sample to sample, so the value from the 1 s experimental subspectrum is used to define the amorphous peaks in the difference and quantitative spectra. We assume these two peaks are symmetric, centered about those well-known shifts, and as shown by the four different 1 s EASY subspectra in Figures 5 and 6, the two components reasonably represent the experimental spectrum. These results are representative of what was encountered for all samples.

DOI: 10.1021/acs.macromol.5b00475
Macromolecules 2015, 48, 3040−3048

The same process is repeated for the difference "rigid only" spectra, i.e., two components centered at the two known chemical shifts (excluding the monoclinic component at 34.4 ppm if present) are used to represent that line shape, as shown in the bottom traces of Figures 5 and 6. Of these two, one is the crystalline all-trans segments, the peak shape for which is well-known and easy to fit, while the second is the constrained amorphous component. In addition to fitting the EASY difference spectrum to these two components, we verified the position of the constrained amorphous peak by short contact time CP experiments, which are shown by Figure S2 in the Supporting Information. The position and shape of the amorphous component in 10, 50, and 100 μs contact time CP experiments, as well as the crystalline component, are almost identical to those found in the EASY "rigid-only" difference spectrum. Of course, the EASY approach is quantitative while CP cannot be considered quantitative due to its dependence on multiple relaxation parameters. Additional confirmation of these individual component assignments is shown in Figures S3 and S4. Figure S3 demonstrates that the rigid amorphous component is required in order to fit the EASY rigid-only subspectra, while Figure S4 shows that the line shape obtained in the mobile-only 1 s delay EASY subspectra agrees with that obtained in a ^{13}C saturation recovery spin−lattice relaxation experiment using a 1 s recovery time.

The final step is to see how these four components, extracted two at a time from the two resolved subspectra, fit the 2000 s line shape from the first part of each EASY experiment. The four components extracted from the two subspectra (mobile-only and rigid-only) are used without modification to their position or area to fit the total intensity 2000 s EASY spectrum. The sequence of data analysis is critical, as attempting to fit the 2000 s spectrum first, without the benefit of the resolved EASY subspectra, would be problematic. As shown in Figures 5 and 6, the agreement between the fits and the experiment are good. Again, the 2000 s EASY spectrum is never analyzed *a priori*. Voigt functions were used for all line shape components shown in Figures 5 and 6 as well as the other PE results. Typically, the Lorentzian:Gaussian (ratio) used for the crystalline all-trans peak was 2:1, while for the remaining peaks a ratio of 0.5−1 was typical. All-trans signals were centered at 32.8 ppm, while the amorphous signals were centered in the range 30.8−31.7 ppm, depending on the value measured in the 1 s EASY mobile-only subspectrum.

The total crystalline fraction reported in Table 2 is the sum of all-trans rigid orthorhombic and monoclinic crystalline fractions and is in general agreement with (first heat) DSC crystallinity results as shown by the graph in Figure S1 of the Supporting Information; the largest deviation between the two methods is ca. 10%. Note that the NMR percent crystallinity is assigned here as the relative fraction of total intensity derived *only* from the rigid all-trans line shape. The interface intensity of sample L-400 (Figure 5, right column) was found to be significantly higher than that of sample L-45 (left column). Using the approach described above and exemplified in Figures 5 and 6, the amounts of each of the four components (or five in the cases where a monoclinic crystalline fraction was detected) were determined for the PE's in Table 1. The results are summarized in Table 2 and depicted graphically for the mobile all-trans and constrained amorphous fractions versus M_w in Figure 7. The total interface fraction (mobile all-trans + constrained amorphous) exhibits a near linear relationship with M_w for the linear PE's but exhibits significant deviation from

Table 2. Phase Composition and Interface Content in PE's, Extracted from the Modified-EASY Experiment[a]

sample	M_w (kg/mol)	total crystalline	mobile all-trans	constrained amorphous
L-45	45	74.6 ± 0.4	3.9 ± 0.1	1.4 ± 0.5
L-165	165	59.6 ± 0.8	3.7 ± 0.1	3.4 ± 0.2
L-184	184	51.7 ± 0.3	5.3 ± 0.1	3.9 ± 0.3
L-241	241	56.9 ± 0.7	5.2 ± 1.4	4.4 ± 0.6
L-289	289	50.6 ± 1.6	5.3 ± 0.3	7.8 ± 0.9
L-294	294	49.6 ± 2.0	5.4 ± 0.2	6.9 ± 0.7
L-400	400	50.5 ± 0.8	8.1 ± 0.5	6.4 ± 0.6
U-1466	1466	54.1 ± 0.5	7.6 ± 0.2	5.8 ± 0.3
SCB-43-h	43	63.8 ± 0.2	5.3 ± 0.9	6.4 ± 0.2
SCB-146-b	146	40.0 ± 0.5	8.2 ± 0.5	3.8 ± 0.2
SCB-148-o	148	44.6 ± 0.6	11.6 ± 0.9	1.9 ± 0.6
SCB-184-o	184	41.6 ± 0.3	9.0 ± 0.7	5.4 ± 0.1
LCB-152	152	48.3 ± 0.8	5.7 ± 0.1	6.0 ± 0.6
LCSC-284	284	35.9 ± 0.5	12.4 ± 0.1	7.5 ± 0.4
LCSC-627	627	41.3 ± 0.5	13.3 ± 0.3	7.1 ± 0.3

[a]The total amorphous content, while not listed, follows from the reported total crystalline percentage. Total crystalline percentages do not include the mobile all-trans contribution. The reported ranges in each data point correspond to one standard deviation arising from deconvoluting each set of EASY subspectra three times.

that relationship once short-chain branching is introduced for the same M_w, as shown in both Figures 7 and 8. Figure 7a and Table 2 show that most of this increase arises from the increased mobile all-trans fraction of the SCB relative to their corresponding molecular-weight linear analogues. Moreover, the UHMWPE synthesized using Ziegler−Natta catalysis (U1466), and the LCSC samples, are clearly outliers relative to the base linear M_w dependence. Figure 8 shows that the effect of introducing short-chain branches, whether butene, hexene, or octene-generated and whether on a linear polymer or in a LCB polymer, is to increase the interfacial content per unit molecular weight. We note with interest that the two LCB polymers with SCB's (LSCS) have by a wide margin the largest interfacial content. The single "pure" LCB data point, denoted by the "+" in Figure 8 at a M_w = 161K, has an interfacial content that lies between the general trend exhibited by the linear and short-chain branched PE's, as might be expected given its very low 0.34 branches/10000 total carbons. However, the extra detail afforded by Figure 7a,b shows that this LCB has a higher constrained amorphous content than the corresponding linear or SCB PE per unit molecular weight.

To clarify, potential confusion could arise between the "constrained amorphous" term, as used here to denote that fraction of amorphous polymer that does not survive the ^{13}C T_1 filter used in the EASY experiments, and other constrained or rigid amorphous phases previously discussed by others [refs 21 and 35 and references therein]. Other discussions of novel uses of T_{1C} filters have also appeared, targeting identification of intermediate phases.[36] Proton dipolar couplings have been used as the discriminatory parameter in ^{1}H spin−spin relaxation, spin-diffusion, and multiple-quantum echo methods, all of which rely on chain dynamics in the 10^4−10^5 s^{-1} spectral density regime, uniquely different than the effective spin−lattice spectral densities (~10^8 s^{-1}) required for the ^{13}C T_1 relaxation filter used here. It is likely that the T_{1C} selection is a stronger filter in terms of the subset of population it selects relative to the proton methods cited above.

DOI: 10.1021/acs.macromol.5b00475
Macromolecules 2015, 48, 3040−3048

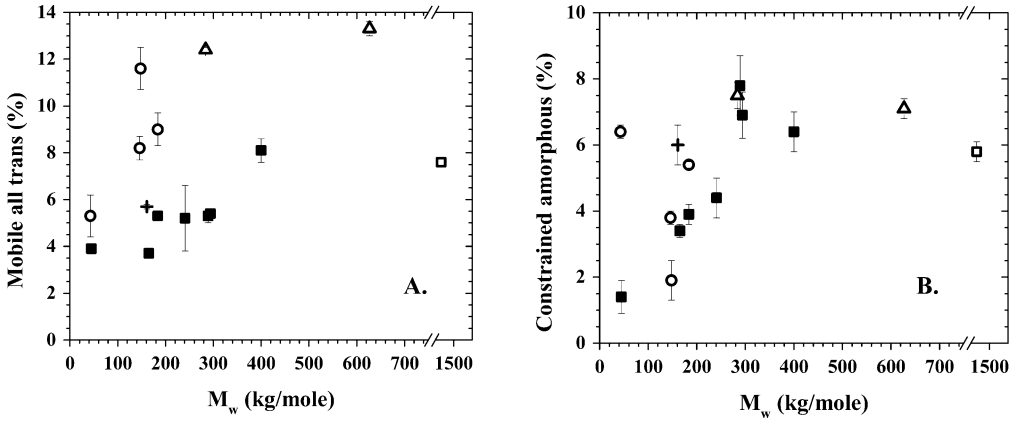

Figure 7. Graphical summary of data from modified-EASY experiments demonstrating how interfacial morphology varies with PE chain length and chain architecture: (a) mobile all-trans chain fraction; (b) constrained amorphous chain fraction (■, linear PE; ○, SCB; +, LCB; △, LCSC).

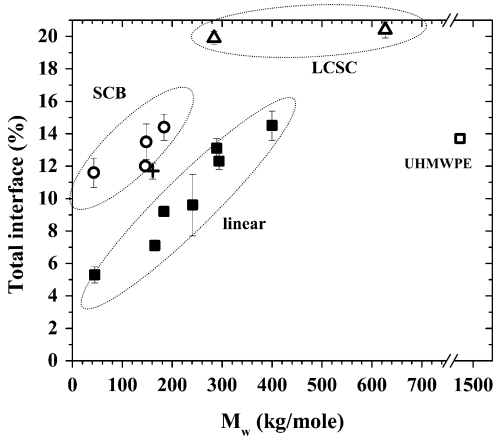

Figure 8. Results from modified-EASY experiments demonstrating molecular-weight dependencies of the total interfacial content (mobile all-trans plus constrained amorphous) for different PE chain topologies (■, linear PE; ○, SCB; +, LCB; △, LCSC). Note the unique grouping according to PE chain architecture.

As discussed in the Experimental Section and Introduction, the materials used here were essentially all reactor fluffs. Obviously, thermal history, polymerization temperatures, reactor pressure, and other variables can contribute to perturbations in final sample morphology. All of these variables were controlled in facilities capable of making commercial-grade polymers within narrow specification ranges, and we believe that the method introduced in this contribution is capable of accurately representing the total contribution of structural variables to interfacial variations. We believe that the aforementioned variables certainly can contribute to changes within a polymer class, but Figure 8 suggests that a major factor in shifting polymer chain types to new interfacial contents is the presence of branches and the type of branches.

■ CONCLUSIONS

The double acquisition EASY solids NMR pulse sequence, modified to suppress nuclear Overhauser effects, revealed that the amounts of interfacial phase regions, defined as the sum of the constrained amorphous and mobile all-trans chain contents, vary in linear PE's according to molecular weight in a linear fashion. However, more complex PE chain architectures have significantly larger interfacial content. Specifically, the introduction of branching increases the amount of mobile all-trans and constrained amorphous chains per unit molecular weight, with significant deviations from linear PE trends observed for short-chain branched PE, and especially so for long-chain branched PE that also contained small amounts of short-chain branching. The type of comonomer used in ethylene/α-olefin copolymers appears to have little impact on the interfacial content, although more exhaustive future studies will be required to confirm what these initial data suggest. Essentially all PE materials used in this work were reactor fluff polymers. Now that an accessible method exists to reliably determine the details of the interfacial chain compositions and their overall content, continuing work will focus on determining the degree to which the interface between the crystalline and amorphous domains in PE significantly depends upon additional thermal processing steps, and how it might meaningfully influence physical and mechanical properties.

■ ASSOCIATED CONTENT

Ⓢ Supporting Information

DSC crystallinity results and representative solid state NMR control experiments to confirm line shape assignments. This material is available free of charge via the Internet at http://pubs.acs.org.

■ AUTHOR INFORMATION

Corresponding Author

*E-mail jeff.white@okstate.edu (J.L.W.).

Present Address

P.J.D.: Chevron Phillips Chemical Co., Bartlesville, OK.

Notes

The authors declare no competing financial interest.

■ ACKNOWLEDGMENTS

The authors gratefully acknowledge support of this project by the National Science Foundation (GOALI Grant DMR-1203848) and the Chevron Phillips Chemical Company LP. Dr. Youlu Yu is gratefully acknowledged for help in acquiring the SEC-MALS data.

■ REFERENCES

(1) Malpass, D. B. *Introduction to Industrial Polyethylene: Properties, Catalysts, and Process*; Scrivener Publishing LLC: Salem, MA, 2010.

(2) Peacock, A. J. *Handbook of Polyethylene*; Marcel Dekker, Inc.: New York, 2000.

DOI: 10.1021/acs.macromol.5b00475
Macromolecules 2015, 48, 3040−3048

(3) Shamiri, A.; Chakrabarti, M. H.; Jahan, S.; Hussain, M. A.; Kaminsky, W.; Aravind, P. V.; Yehye, W. A. The Influence of Ziegler-Natta and Metallocene Catalysts on Polyolefin Structure, Properties, and Processing Ability. *Materials* **2014**, *7*, 5069−5108.
(4) Mead, W. T.; Desper, C. R.; Porter, R. S. Physical and Mechanical Properties of Ultra-Oriented High-Density Polyethylene Fibers. *J. Polym. Sci., Polym. Phys. Ed.* **1979**, *17*, 859−892.
(5) Phillips, T. L.; Hanna, S. Simulation of the Mobile Phase of Polyethylene. *Polymer* **2005**, *46*, 11035−11050.
(6) Lee, S.; Rutledge, G. C. Plastic Deformation of Semi-crystalline Polyethylene by Molecular Simulation. *Macromolecules* **2011**, *44*, 3096−3108.
(7) Ghazavizadeh, A.; Rutledge, G. C.; Atai, A. A.; Ahzi, S.; Remond, Y. Micromechanical Characterization of the Interphase Layer in Semi-crystalline Polyethylene. *J. Polym. Sci.* **2013**, *51*, 1228−1243.
(8) Doskocilova, D.; Schneider, B.; Jakes, J.; Schmidt, P.; Baldrian, J. ^{1}H Nuclear Magnetic Resonance Characterization of Internal Motions in the Amorphous Phase of Low-Density Polyethylene. *Polymer* **1986**, *27*, 1658−1664.
(9) Eckman, R. R.; Henrichs, P. M.; Peacock, A. J. Study of Polyethylene by Solid State NMR Relaxation and Spin Diffusion. *Macromolecules* **1997**, *30*, 2474−2481.
(10) Hansen, E. W.; Kristiansen, P. E.; Pedersen, B. Crystallinity of Polyethylene Derived From Solid-State Proton NMR Free Induction Decay. *J. Phys. Chem. B* **1998**, *102*, 5444−5450.
(11) Kaji, A.; Ohta, Y.; Yasuda, H.; Murano, M. Phase Structure Analysis of Ultra High-Molecular Weight Polyethylene Fibers by Solid State High Resolution NMR. *Polym. J.* **1990**, *22*, 455−462.
(12) Kitamaru, R.; Horii, F.; Zhu, Q. The Phase Structure of High-Pressure-Crystallized Polyethylene. *Polymer* **1994**, *35*, 1187−1181.
(13) Cheng, J.; Fone, M.; Reddy, V. N.; Schwartz, K. B.; Fisher, H. P.; Wunderlich, B. Identification and Quantitative Analysis of the Intermediate Phase in a Linear High-Density Polyethylene. *J. Polym. Sci., Part B: Polym. Phys.* **1994**, *32*, 2683−2693.
(14) Kuwabara, K.; Kaji, H.; Horii, F. Solid-State ^{13}C NMR Analysis for the Structure and Molecular Motion in the α-Relaxation Temperature Region for Metallocene-Catalyzed Linear Low-Density Polyethylene. *Macromolecules* **2000**, *33*, 4453−4462.
(15) Zhang, L.; Hansen, E. W.; Helland, I.; Hinrichsen, E.; Larsen, A.; Roots, J. Crystallinity in Ethene-1-Hexene Copolymer Determined by ^{1}H and ^{13}C NMR. A Comparative Study. *Macromolecules* **2009**, *42*, 5189−5195.
(16) Kuwabara, K.; Kaji, H.; Horii, F. Solid State ^{13}C NMR Analysis of the Crystalline − Noncrystalline Structure for Metallocene-Catalyzed Linear Low-Density Polyethylene. *Macromolecules* **1997**, *30*, 7516−7521.
(17) Chen, Q.; Kurosu, H. Solid-State NMR Studies on Semi-Crystalline Polymers. In *Annual Reports on NMR Spectroscopy*; Webb, G., Eds.; Elsevier Ltd.: London, 2007; Vol *61*, pp 247−281.
(18) Yamanobe, T.; Uehara, H.; Kakiage, M. Practical NMR Analysis of Morphology and Structure of Polymers. In *Annual Reports on NMR Spectroscopy*; Webb, G., Eds.; Elsevier Ltd.: Oxford, 2010; Vol. *70*, pp 203−239.
(19) Yao, Y.; Jiang, S.; Rastogi, S. ^{13}C Solid State NMR Characterization of Structure and Orientation Development in the Narrow and Broad Molar Mass Disentangled UHMWPE. *Macromolecules* **2014**, *47*, 1371−1382.
(20) Kiho, H.; Peterlin, A.; Geil, P. H. Polymer Deformation. VI. Twinning and Phase Transformation of Polyethylene Single Crystals as a Function of Stretching Direction. *J. Appl. Phys.* **1964**, *35*, 1599.
(21) Litvinov, V. M.; Kurelec, L. Remarkably High Mobility of Some Chain Segments in the Amorphous Phase of Strained HDPE. *Polymer* **2014**, *55*, 620−625.
(22) Hu, W. G.; Schmidt-Rohr, K. Characterization of Ultradrawn Polyethylene Fibers by NMR: Crystallinity, Domain Sizes and A Highly Mobile Second Amorphous Phase. *Polymer* **2000**, *41*, 2979−2987.
(23) Schmidt-Rohr, K.; Spiess, H. W. *Multidimensional Solid-State NMR and Polymers*; Academic Press: San Diego, CA, 1994.
(24) Chaiyut, N.; Amornsakchai, T.; Kaji, H.; Horii, F. Solid-State ^{13}C NMR Investigation of the Structure and Dynamics of Highly Drawn Polyethylene- Detection of the Oriented Non-Crystalline Component. *Polymer* **2006**, *47*, 2470−2481.
(25) Schmidt-Rohr, K.; Spiess, H. W. Chain Diffusion between Crystalline and Amorphous Regions in Polyethylene Detected by 2D Exchange ^{13}C NMR. *Macromolecules* **1991**, *24*, 5288−5293.
(26) Hu, W. G.; Boeffel, C.; Schmidt-Rohr, K. Chain Flips in Polyethylene Crystallites and Fibers Characterized by Dipolar ^{13}C NMR. *Macromolecules* **1999**, *32*, 1611−1619.
(27) Jaeger, C.; Hemmann, F. EASY: A Simple Tool for Simultaneously Removing Background, Deadtime and Acoustic Ringing in Quantitative NMR Spectroscopy − Part I: Basic Principle and Applications. *Solid State Nucl. Magn. Reson.* **2014**, *57*−*58*, 22−28.
(28) Lohmeyer, S. *Die speziellen Eigen-schaften der Kunststoe*; Expert Verlag: Grafenau, 1984. Also: Tzavalas, S.; Macchiarola, K.; Gregoriou, V. G. *J. Polym. Sci., Polym. Phys.* **2006**, *44*, 914−924.
(29) Yu, Y.; DesLauriers, P. J.; Rohlfing, D. C. *Polymer* **2005**, *46*, 5165−5182.
(30) Randall, J. C. *J. Macromol. Sci., Rev. Macromol. Chem. Phys.* **1989**, *C29*, 201.
(31) Kitamaru, R.; Horii, F.; Murayama, K. Phase Structure of Lamellar Crystalline Polyethylene by Solid-State High-Resolution ^{13}C NMR: Detection of the Crystalline-Amorphous Interphase. *Macromolecules* **1986**, *19*, 636−643.
(32) Earl, W. L.; VanderHart, D. L. Observations in Solid Polyethylene by Carbon-13 Nuclear Magnetic Resonance with Magic Angle Sample Spinning. *Macromolecules* **1979**, *12*, 762−767.
(33) Tonelli, A. E. *NMR Spectroscopy and Polymer Microstructure: The Conformational Connection*; VCH Publishers: New York, 1989; Chapter 11 and references therein.
(34) VanderHart, D. L. Influence of Molecular Packing on State-State ^{13}C Chemical Shifts: The n-Alkanes. *J. Magn. Reson.* **1981**, *44*, 117−125.
(35) Barenwald, R.; Goerlitz, S.; Godehardt, R.; Osichow, A.; Tong, Q.; Krumova, M.; Mecking, S.; Saalwachter, K. Local Flips and Chain Motion in Polyethylene Crystallites: A Comparison of Melt-Crystallized Samples, Reactor Powders, and Nanocrystals. *Macromolecules* **2014**, *47*, 5163−5173.
(36) Mowery, D. M.; Harris, D. J.; Schmidt-Rohr, K. Characterization of a Major Fraction of Disordered All-Trans Chains in Cold-Drawn High-Density Polyethylene by Solid-State NMR. *Macromolecules* **2006**, *39*, 2856−2865.

DOI: 10.1021/acs.macromol.5b00475
Macromolecules 2015, 48, 3040−3048